ADVANCED FUNCTIONAL MATERIALS

www.afm-journal.de

Micro Light-Emitting Diodes for Display and Flexible Biomedical Applications

*Han Eol Lee, Jung Ho Shin, Jung Hwan Park, Seong Kwang Hong, Sang Hyun Park, Seung Hyung Lee, Jae Hee Lee, Il-Suk Kang, and Keon Jae Lee**

Inorganic-based micro light-emitting diodes (μLEDs) have witnessed significant improvements in terms of display and biomedical applications, which can shift the paradigm of future optoelectronic systems. In particular, μLED displays are on the verge of becoming the next big interface platform for visual communications, expanding to various internet of things and wearable/bioapplications. Novel μLED concepts need to be upgraded to be able to satisfy their potential optoelectric applications, such as virtual reality, smart watches, and medical sensors for individual computing in this hyperconnected society. Here, representative progresses in the field of flexible μLEDs are reviewed with regard to device structures, massive μLED transfers, methods for performance enhancement, and applications.

1. Introduction

Inorganic-based micro light-emitting diodes (μLEDs) have been spotlighted as a strong candidate to replace active-matrix organic light-emitting diodes and liquid crystal displays (LCDs) due to their excellent light properties (e.g., hue, contrast, and brightness), fast response time, outstanding power efficiency, and stability.[1–9] The μLED displays with chip-based transfer are already on the verge of commercialization by successfully demonstrating millions of tiny LED pixels in a display panel.[10,11] The μLED fields are currently expanding to various wearable, internet of things (IoT), and biomedical applications such as virtual reality (VR) applications, smart watches, and medical sensors for hyperconnected society.[12–22] In addition, flexible μLEDs have attracted a lot of attentions, because it can be applied to curvilinear or dynamic skin surfaces, clothes, and automobiles to provide user-friendly and biocompatible optoelectronics based on human–machine interface.[1,14,17,23–28]

μLED designs are widely classified into two types: chip-based μLEDs (transferring packaged red-green-blue unit) and thin-film μLEDs (having thickness less than 5 μm). A number of researches in the industry and at universities have developed the chip-based μLED displays and biomedical devices.[16,20,29–32] Although the assembly process for LED digital signage is well established based on the conventional LED technologies, chip-based μLED display has a critical limitation in the mass production of low-cost consumer TVs caused by handling millions of individual chip transfer.[22,33,34] Since chip-based μLED displays are already a mature technology for outdoor LED screens, this review will not discuss this in detail. On the contrary, thin-film μLEDs are considered as a powerful solution to reduce the cost of TV due to rapid and inexpensive mass transfer over ten thousands of μLEDs in one time.[10,22,35–37] Several transfer techniques based on van der Waals force, electrostatic, and magnetic adsorption have been reported.[25,38–48] However, a lot of challenges still have to be solved to demonstrate outstanding resolution, large-scale registration, and remarkable transfer yield for thin-film μLED displays.

The structure and the packaging technology of the thin-film μLEDs are the important factor for the device performance, reliability, and productivity. The device structure determines the overall LED characteristics including power efficiency, brightness, and thermal stability, which are critical factors for display and flexible biomedical applications.[23,49–57] Various types of thin-film μLEDs (e.g., lateral structured μLED, vertical structured μLEDs, and flip chip lateral structured μLED) have been exploited for strategies of enhancing μLED performance.[23,49,56,58–61] Packaging technology, related to the interconnection of transferred μLEDs to other electronic components and their protection from the external stress, is also crucial for fully functional optoelectronic systems.[62–69] A number of packaging technologies have been investigated including metal wiring,[70,71] soldering,[72–74] flip chip bonding,[75–80] and anisotropic conductive film (ACF) bonding.[60,61] Metal wiring and soldering are simple processes, but unsuitable for high resolution display.[81,82] Flip chip bonding is preferred due to

Dr. H. E. Lee, J. H. Shin, Dr. S. K. Hong, S. H. Park, S. H. Lee, J. H. Lee, Prof. K. J. Lee
Department of Materials Science and Engineering
Korea Advanced Institute of Science and Technology (KAIST)
291 Daehak-ro, Yuseong-gu, Daejeon 34141, Republic of Korea
E-mail: keonlee@kaist.ac.kr

Dr. J. H. Park
Department of Mechanical Engineering
University of California
Berkeley, CA 94720, USA

Dr. I.-S. Kang
National Nanofab Center
Korea Advanced Institute of Science and Technology (KAIST)
291 Daehak-ro, Yuseong-gu, Daejeon 34141, Republic of Korea

The ORCID identification number(s) for the author(s) of this article can be found under https://doi.org/10.1002/adfm.201808075.

DOI: 10.1002/adfm.201808075

its short process time and reliable integration of microsized LEDs.[67,75] ACF bonding is favorable for high resolution and efficient μLED packaging without the additional metallization process.[61,66,83,84]

Here, we introduce the overview of thin-film based μLED technology for high resolution display and biomedical applications. Recent progress in the field of thin-film μLEDs is classified into five main categories: (i) research trends of μLED technology, (ii) device structure of μLEDs, (iii) μLED transfer methods, (iv) strategies for performance enhancement, and (v) potential research areas. μLED applications such as next-generation displays, wearable optoelectronics, optogenetic/trichogenic biostimulators, and healthcare biomedical sensors will be discussed.[85–88]

2. Research Trends of μLED Technology

2.1. Comparison of μLED Technology with Other Displays

High-resolution displays using microsized pixels have been considered as a tremendous breakthrough in the display industry.[73,89,90] Although LCD and OLED have dominated the major display market, μLEDs are believed to present outstanding performance beyond conventional displays.[37,91] As tabulated in **Figure 1**, μLEDs have advantages of excellent image quality, superior stability and high form factor compared to LCD and OLED. Self-emissive μLEDs could simplify the display architecture and decrease the device thickness due to the absence of polarizers, color filters, backlight units, and thick encapsulation layers. μLED displays with infinite contrast ratio and superb luminous efficacy exhibited higher brightness (100 000 cd m^{-2}) than that of LCD and OLED. μLED showed long lifetime of over 10 years and wide temperature range, from −100 to 120 °C; these qualities were attributed to highly stable inorganic III–V compounds. On the other hand, OLED presented screen burn-in and short life span of four years due to the thermal/humid instability of organic materials. In addition, μLEDs have great potentials to produce high-quality images because of their fast response time (≈5×10^4 times shorter than that of OLEDs), high color reproduction rate of 140%, and wide view angle.[92,93] At identical pixel number and light intensity, the power efficiency of a μLED display was 77 and 4 times higher than those of LCD and OLED displays, respectively.[94] Based on these excellent characteristics, μLED is considered as a promising light source for future displays, like ultrathin UHD TVs, flexible and biomedical applications by overcoming the limitations of previously displays. However, the μLED still have critical issues to be overcome such as low yield ratio of mass transfer techniques, lack of efficient pixel repair method, and limited resolution of packaging process.

Figure 2 shows the development prospective for μLED displays regarding pixel pitch and density. Generally, inorganic-based mini LEDs (chip size of hundreds of micrometers) have been widely used for large display including outdoor signage, cinema screens, and video walls. The fine pitch display market has been preempted by LCDs and OLEDs, which have been developed for decades of optimizations. However, these technologies showed long-term instability and low-resolution limit for display applications with short viewing distance (e.g., smart glasses, watches, and mobile devices).[92–95] Therefore, μLED is considered as a candidate to replace OLED and LCD, because of its remarkable environmental stability and high resolution over 1000 pixel per inch (PPI).[9,75] It is expected that μLEDs can be used to realize ultrahigh-resolution displays for next-generation AR and VR applications, fulfilling consumer requirements for advanced displays.[22,67,96]

Han Eol Lee received his B.S., M.S., and Ph.D. degrees in materials science and engineering from KAIST in 2013, 2015, and 2018, respectively. Currently, he is a BK21 Plus postdoctoral research associate in the Department of Materials Sciences and Engineering at KAIST. His research topics are thin-film microLEDs, flexible/wearable electronics, and laser material interaction for flexible full-color microLED displays.

Jung Ho Shin is a Ph.D. candidate in materials science and engineering at KAIST. He received his B.S. degree in materials science and engineering from Hanyang University in 2016 and M.S. degree from KAIST in 2018. His research topic includes the development of the inorganic-based flexible optoelectronics for biomedical applications.

Keon Jae Lee received his Ph.D. in materials science and engineering at University of Illinois, Urbana Champaign (UIUC). During his Ph.D., he was involved in the first coinvention of "flexible single-crystalline inorganic electronics," using top-down semiconductors and soft lithographic transfer. Since 2009, he has been a professor in the Department of MSE at KAIST. His current research topics are self-powered flexible electronic systems including energy harvester, IoT sensor, microLEDs, large scale integration, memory, and laser material interaction for biomedical and flexible applications. In addition, he is a cofounder of a spin-off company, FRONICS Ltd., to commercialize his achievements.

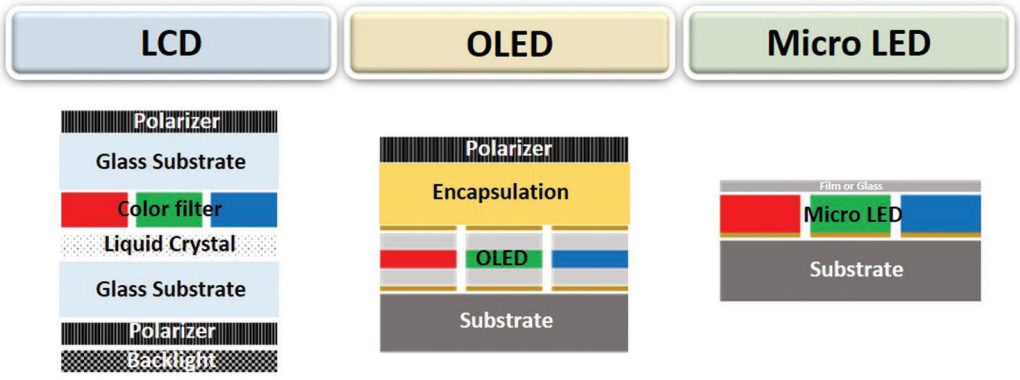

	LCD	OLED	Micro LED
Emission Type	Backlight/LED (thick)	Self-emissive (thin)	Self-emissive (thin)
Contrast Ratio	5000 : 1	∞	∞
Luminous Efficacy	Medium (~ 65 lm W^{-1})	Low (~ 20 lm W^{-1})	High (~ 100 lm W^{-1})
Brightness (cd/m^2)	3000	1500	100,000
Life Span	5 ~ 8 years	~ 4 years	> 10 years
Response Time	5 ms	110 µs	~ 0.2 ns
Operating Temperature (°C)	0 ~ 60	-50 ~ 70	-100 ~ 120
Color Rendering	75% NTSC	> 100% NTSC	140% NTSC
Viewing Angle	Poor (~ 100 °)	Best (~ 140 °)	Best (~ 140 °)
Power Consumption (320×320 pixels, 350 cd/m^2)	3.1 W	200 mW	40 mW
Remarks	Afterimage	Burn-in image, Unstable (heat, humidity)	Stable (heat, humidity)

Figure 1. Comparison of liquid crystal display (LCD), organic light-emitting diode (OLED) and inorganic-based micro light-emitting diode (µLED). Reproduced with permission.[23] Copyright 2018, Wiley-VCH.

2.2. Core Element Technologies for µLED

Many researchers have studied µLEDs with regard to device structure, transfer, and packaging techniques to increase their performance, production yield, and pixel density. To solve a lot of commercialization issues, a systematic approach of µLED research needs to be established by considering the connectivity between target application and core elemental technology.[22,34] **Figure 3** provides a technical overview of µLED developments. First, the target application should be determined to decide the detail specification of optimum elemental technologies. This objective setting is important for the µLED design, such as device thickness, materials, and configuration because of its strong dependence on the targeted usage. According to the µLED target and design, corresponding elemental core technologies such as device structure, transfer, and packaging technologies can be optimized for the required µLED characteristics.

Figure 4 presents characteristics comparisons of chip-based µLEDs and thin-film µLEDs with vertical/lateral structures. Chip-based µLEDs with a thickness over 50 µm have been used for full-color TVs, however these technologies do not satisfy the standards of low-cost and high-speed fabrication, due to millions of individual chip transfer. Instead, a plausible solution is thin-film based µLEDs, which can increase transfer speed by using cost-effective, fast, and massive transfer in one time. Thin-film µLEDs are classified into two types depending on the device structure: lateral µLEDs (LLEDs)[97,98] and vertical µLEDs (VLEDs).[99,100] LLEDs can be fabricated by simple flip-chip processes, however, they have drawbacks of low optical power, and high heat generation. On the other hand, VLEDs have merits of outstanding output efficiency, heat stability, and simple electrode architecture.

µLED transfer from a mother substrate to a target substrate is regarded as one of the most important technologies for large-scale and high-pixel full-color displays.[101] As shown

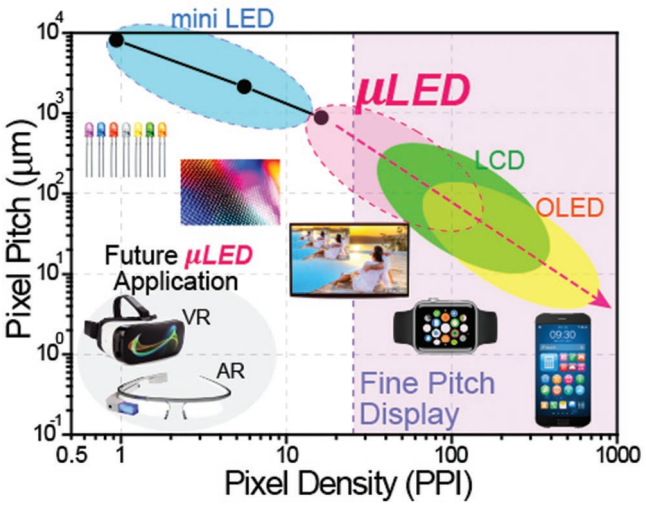

Figure 2. Prospective of μLEDs for fine pitch display, which has been occupied by LCD and OLED displays.

in **Figure 5**, several transfer methods such as electrostatic transfer,[102,103] elastomer stamping,[25,38,39,41,42,44,46–48] laser-assisted transfer,[104–106] electromagnetic transfer,[40,45] pressure-based transfer, and ACF adhesive transfer methods have been developed to assemble μLEDs.[23,49] Electrostatic transfer utilizes voltage-induced adhesion to pick up μLEDs from a mother substrate and subsequently release them onto a target substrate.[102,103] Elastomer stamping is used to transfer the thin-film μLEDs utilizing the adhesion force of polydimethylsiloxane (PDMS).[25,38,39,41,42,44,46–48] Laser-assisted transfer is developed for selective μLED printing upon laser irradiation on the light-reactive layers.[104–106] Electromagnetic transfer detaches μLEDs from the mother wafer using a magnetic attraction between a transfer module and ferromagnetic layers on μLEDs.[43,45] The microvacuum-based transfer method picks up and releases subminiature LED chips by changing a vacuum pressure of the transfer module, which conformally contacts μLED surfaces. Individual vacuum pressure control of each device enables large-scale and selective μLED transfer without any adhesive and heating/compressing process. ACF adhesive transfer bonds between thin-film μLEDs and a target substrate by a simple thermos-compressive process. This simple technique shows high reliability and compatibility with large-scale processes, regardless of lateral and vertical μLED structures.[61,83,84] However, the above-mentioned transfer techniques still have many obstacles, such as μLED damages, misalignment, slow speed, irreversible bonding, and repairing issues.

Solution to defective pixels is essential to acquire perfect image of μLED display. One approach is an individual chip replacement after μLED transfer. If dead pixels are found during inspection, new μLEDs are selectively attached beside damaged ones. This method is only possible if transfer yield is sufficiently high, otherwise an enormous time-consumption is inevitable due to its individual repairing. The other method is a dual μLED transfer into each display pixel without postreplacement process. In this case, if one μLED unit is broken or missing, the pixel can still maintain its illuminance by converting input current to adjacent μLED unit.

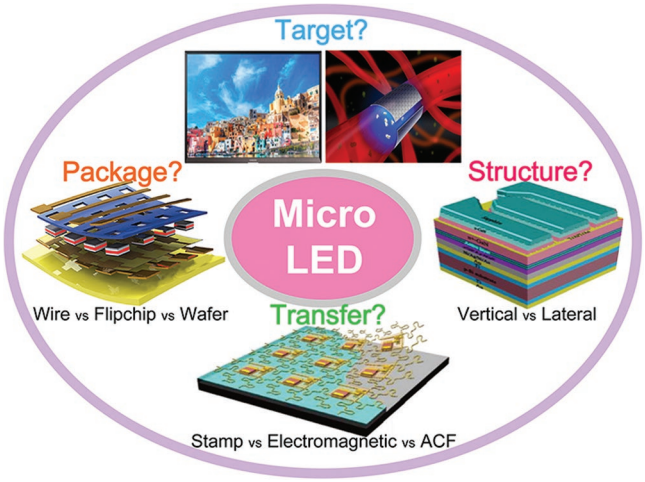

Figure 3. Significant factors for μLED applications, which include target device, structure, packaging, and transfer technologies. Top image: Reproduced with permission.[135] Copyright 2012, Dove Medical Press Ltd. Left image: Reproduced with permission.[60] Copyright 2014, Royal Society of Chemistry. Right image: Reproduced with permission.[136] Copyright 2012, OSA Publishing. Bottom image: Reproduced with permission.[122] Copyright 2017, Wiley-VCH.

Packaging is another crucial technology to realize fully operational optoelectronic systems, enabling the interconnection of core and peripheral electronics.[60,83,84,107–112] Various packaging methods such as wire, flip-chip, and wafer bonding have been developed.[1,70,71,75–80,113] Wire bonding requires heat, ultrasonic vibration or pressure to form interconnections between μLEDs and other components. However, this method had challenges of limited resolution and wire fragility.[81] Flip-chip and wafer bonding have been utilized for μLED displays due to their high production yield and outstanding operation reliability. On the contrary, these methods were unsuitable for high-yield fine-pitch displays with tens of micrometers resolution.[75,78] ACF has been proposed as a powerful packaging medium that can transfer and simultaneously interconnect thin-film μLEDs to flexible substrates through thermocompressive bonding. This packaging technology exhibited moderate transfer area, high resolution capability, and outstanding operation reliability for high performance μLEDs.[108–112]

3. Key Technologies for High-Performance Thin-Film μLEDs

3.1. Device Structure of μLEDs

The device structure of thin-film μLEDs is a critical factor to improve device performances such as thermal stability, output power, and operation efficiency.[50,57,114] Many researchers have simulated the effects of μLED characteristics according to the device structure. Lee and co-workers theoretically analyzed the temperature distribution of flexible GaN μLEDs via the finite element method (FEM) simulation.[23] **Figure 6** provides comparisons of flexible VLED (f-VLED) flexible LLED (f-LLED). As shown in Figure 6a,b, f-VLED exhibited 100 Kelvin degrees lower junction temperature than that of f-LLED when both thin-film μLEDs

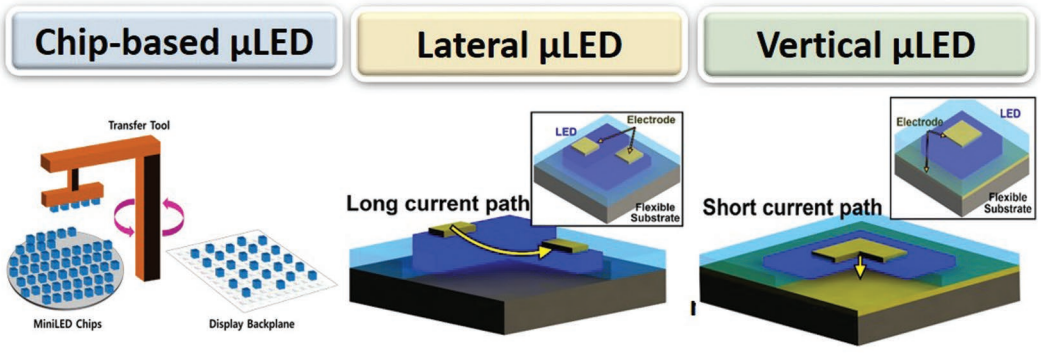

Type	Packaged chip-based LED	Thin-film µLED	
Thickness	> 50 µm	< 5 µm	
Process	High cost & Low speed (1 Chip transfer)	Low cost & High speed (1000 ~ 10000 Chip transfer)	
Power efficiency (Relative $P_{optical}$ at 1 A)	High	Low (1)	High (1.875)
Thermal stability (T at 20 mW mm^{-2} irradiance)	High	Low (428 K)	High (326 K)
Wiring	Complex	Complex	Simple
Light-emitting area	-	Size-dependent	Size-independent

Figure 4. Comparison of chip-based µLED, thin-film lateral-structured µLED (LLED) and thin-film vertical-structured µLED (VLED).

emitted the same optical power of 20 mW mm^{-2}. The generated heat of the f-VLED was distributed by a bottom electrode, while the f-LLED accumulated thermal energy in multiquantum well layers, as depicted in the inset images of Figure 6a,b. Figure 6c displays the calculated temperatures of f-VLED and f-LLED as a function of light irradiance. The heat dissipation of an LED chip is closely related to the emission wavelength shift, power efficiency, and lifespan of the thin-film µLEDs. The temperature difference of flexible µLEDs was proportional to the optical output power, which was 102 Kelvin degrees at 20 mW mm^{-2} irradiance. The excellent thermal stability of the f-VLED was attributed to heat dissipation through the efficient heat sink of the bottom electrode and the short current path inside the LED chip.

Chu et al. experimentally demonstrated µLED performance depending on device structure by investigating the electrical/thermal properties of the GaN LLED and VLED.[114] Figure 6d shows an optical power comparison of an LLED on a sapphire substrate and a thin-film VLED on a metal alloy substrate. The irradiance of the LLED had a maximum value at an injection current of 1000 mA, and decreased due to thermal degradation of the µLED chip when the current was over 1000 mA. By contrast, the thin-film VLED stably operated at high current of 3000 mA without any performance degradation, due to superior thermal diffusivity of the metal substrate. Figure 6e presents *I*–*V* curves of the VLED and the LLED with the same chip size. The LLED had a higher forward voltage (3.4 V) than that of the thin-film VLED (3.0 V), due to its high electrical resistance and current crowding effect during LED operation. As shown in Figure 6f, the thin-film VLED showed negligible changes in light output efficiency, while the extraction efficiency of the LLED was inversely proportional to the chip size despite the scaling down of the µLED chip size.

3.2. Performance Enhancement of µLEDs

Several teams have studied the improvement methods of µLED efficiency. Chip size reduction is a simple strategy of performance enhancement without any additive layers inside the LED chip. **Figure 7** presents performance improving methods of thin-film µLEDs. As shown in Figure 7a, Gong et al. reported size-dependent efficiency of µLEDs including high light output and low junction temperature.[115] Figure 7b indicates that the forward voltage (V_f) of µLEDs was reduced as device dimensions decreased. Furthermore, a small LED with chip size of 20 × 20 µm^2 had not only high irradiance of ≈90 W cm^{-2}, but also low junction temperature of ≈370 K at current density of 4600 A cm^{-2}. These results indicate that chip size reduction

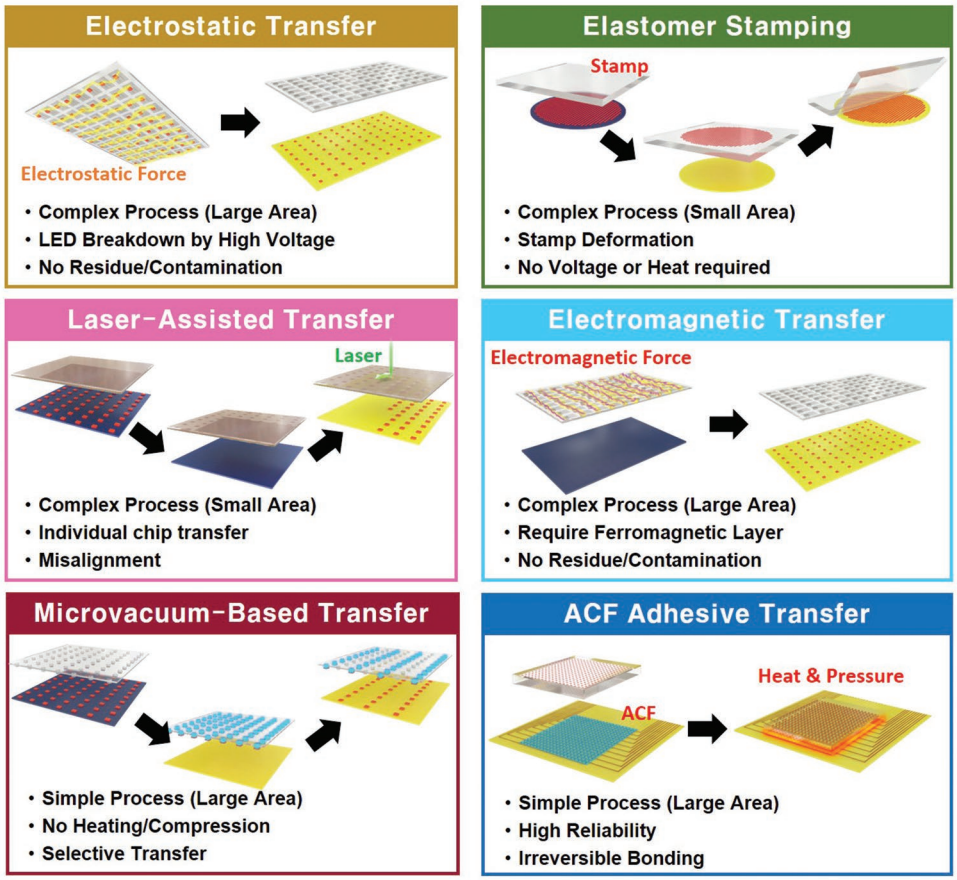

Figure 5. Summary of μLED transfer techniques, including electrostatic transfer, elastomer stamping, laser-assisted transfer, electromagnetic transfer, ACF adhesive transfer, and microvacuum-based transfer methods.

decreased the electrical resistance of the μLED, improving the optical performance and thermal stability.

To enhance the light extraction efficiency, various methods such as patterned sapphire substrate, lens integration, surface texturing, and Bragg reflector implementation on μLEDs have been investigated. Figure 7c presents GaN μLEDs with parabolic nanolenses for light condensing.[116] The lens-integrated μLED had increased light intensity and 30%-decreased divergent angle by minimizing the irregular light diffusion. Figure 7d displays a scanning electron microscope image of a surface-roughened AlGaInP μLED demonstrated by wet etching process (H_3PO_4:HCl = 5:1 for 40 s).[117] As shown in Figure 7e, the external quantum efficiency and the light output power increased by 200% and 150%, respectively, compared to those of conventional μLEDs. Figure 7f represents near-ultraviolet (UV) μLEDs with patterned reflectors to increase light extraction efficiency.[118] The SiO_2/Ta_2O_5-based reflectors in the μLEDs prevented the back reflection of extracted light, increasing the light output power by 40% compared to that of conventional LEDs.

Current spreading layer on an LED chip has been explored to reduce the electrical resistance of μLEDs via metal ohmic contact, annealing process, and modulation of doping concentration. Figure 7g exhibits the specific contact resistance (ρ_c) between an n-type GaN layer and a metal multilayer of Ti/Al/Ni/Au after high-temperature annealing process.[119] The ρ_c of the 750 °C-annealed metal/GaN was ≈50 times lower than that of the 600 °C-annealed sample. Lee et al. reported enhancing effects of μLED properties after using a transparent conducting layer (TCL).[120] An indium-zinc-oxide (IZO)-based TCL enabled fast current spreading and transparent ohmic contact for a GaN μLED, improving the electrical conductance and light output power. Figure 7h,i shows that surface roughened and TCL-coated VLEDs reduced the V_f by 0.22 V and increased light output by 79.3% compared with the untreated conventional VLED.

3.3. Transfer Methods of Thin-Film μLED

Handling of thin-film μLED transfer is a difficult issue for large-scale, low cost, and high-density displays.[41,44,48] The mass transfer of thin-film μLEDs has been intensively investigated since Lee et al. introduced large area and multiple printing of single crystal microstructured semiconductors using PDMS stamp.[39] **Figure 8** shows a technical comparison of μLED transfer. Figure 8a presents an elastomeric stamping method based on kinetical adhesion control by modulating the attaching/detaching rate of a polymeric stamp.[48] After conformal contact between the stamp and the thin-film microstructured semiconductor, the stamp was rapidly peeled up to lift-off the devices from the mother substrate. The exfoliated

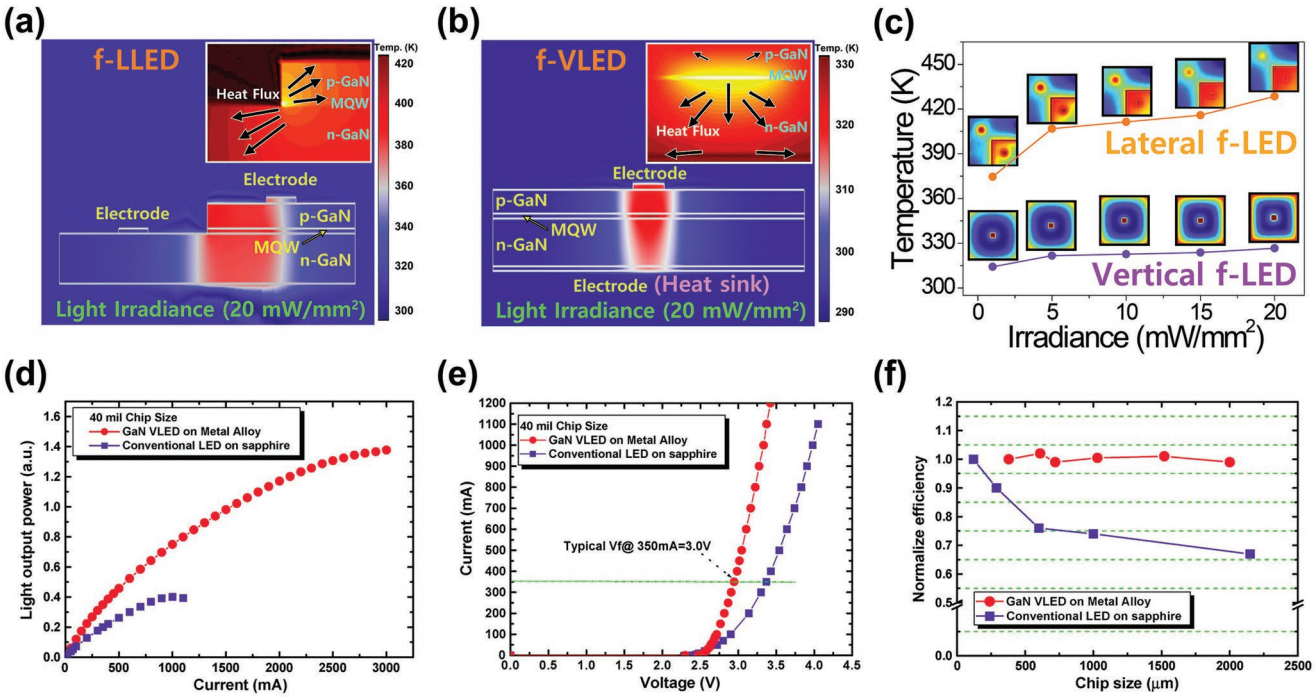

Figure 6. Temperature of a) f-LLED and b) f-VLED, which were theoretically calculated by FEM simulation. The insets show isothermal images of each μLED chip. c) FEM simulated temperature of f-LLED and f-VLED as a function of light output power. Reproduced with permission.[23] Copyright 2018, Wiley-VCH. d) Optical power of GaN f-LLED on sapphire substrate and f-VLED on metal alloy at same chip size. e) *I–V* curves of GaN f-LLED and f-VLED. f) Normalized extraction efficiency values of GaN f-LLED and f-VLED as a function of LED chip size. Reproduced with permission.[114] Copyright 2010, IEEE.

μLEDs were released onto the target substrate by slow detachment of the stamp. Using a PDMS stamp, 6 × 6 thin-film μLED arrays were successfully transferred onto an elongated PDMS substrate, as shown in Figure 8b.[121] The μLED display exhibited stable optical and electrical characteristics under horizontal (≈48%) and diagonal stretching (≈46%) conditions. As illustrated in Figure 8c, Choi et al. reported roll-based elastomer stamping technology, enabling a large-scale, high yield, and rapid transfer process for μLED displays.[122] A stretchable μLED display was integrated with single crystal Si-based thin film transistors (TFTs) on a polymer substrate. The transferred active-matrix (AM) LEDs and TFTs exhibited constant electrical characteristics under elongation of 40%, indicating the mechanical stability of the stretchable μLED display. The elastomeric printing technique, however, was still suffered from low stamp durability and difficulty of precise registration.

ACF, an adhesive transfer medium of thin-film μLEDs, enables not only attachment of μLEDs to a target substrate but also simultaneous interconnection between μLEDs and peripheral devices. Figure 8d represents passive-matrix (PM) f-VLEDs on a polyimide (PI) substrate using ACF as a mass transfer medium.[61] The μLED chips were thermo-compressed at low temperature (190 °C) and moderate pressure (3 MPa), strongly bonding with the bottom electrode by the ACF resin. The cross-sectional SEM image showed deformed conductive balls in the ACF, interconnecting the LED chips to the bottom electrode as shown in the inset of Figure 8d. Figure 8e shows that a self-powered fully flexible μLED system can be realized on a plastic substrate via ACF mass transfer method.[60,123–125] The transferred μLEDs maintained their optical and electrical properties even with a small bending radius of 3 mm. This excellent mechanical stability came from the ACF-induced strong adhesion between the μLED chips and the electrodes.

4. Research Applications of μLEDs

4.1. Display Applications

μLED technology will serve as a platform for large area and high performance display application due to its high contrast ratio, fast response time, and low power consumption.[2–4,6,7,9] Researchers have suggested two strong candidates for realizing full-color red-green-blue (RGB) thin-film μLED displays: (i) color conversion from blue/UV μLEDs using quantum dots (QDs) and (ii) transfer of red, green, and blue μLEDs in three separate processes.[10,126–128] **Figure 9** exhibits various demonstrations of μLED displays. Figure 9a schematically illustrates the fabrication procedures for a full-color μLED display using QD aerosol jet printing.[126,128] QD-dispersed solutions were selectively sprayed on UV μLED arrays in the order of red, green, and blue QDs. QD-based color filters successfully converted the UV light of μLEDs to red, green, and blue light without color mixing. Figure 9b shows a process schematic of a passive-matrix inorganic full-color μLED (PMILED) display using stamping transfer of true RGB μLEDs.[127] Self-emissive full-color μLEDs were separately transferred from the

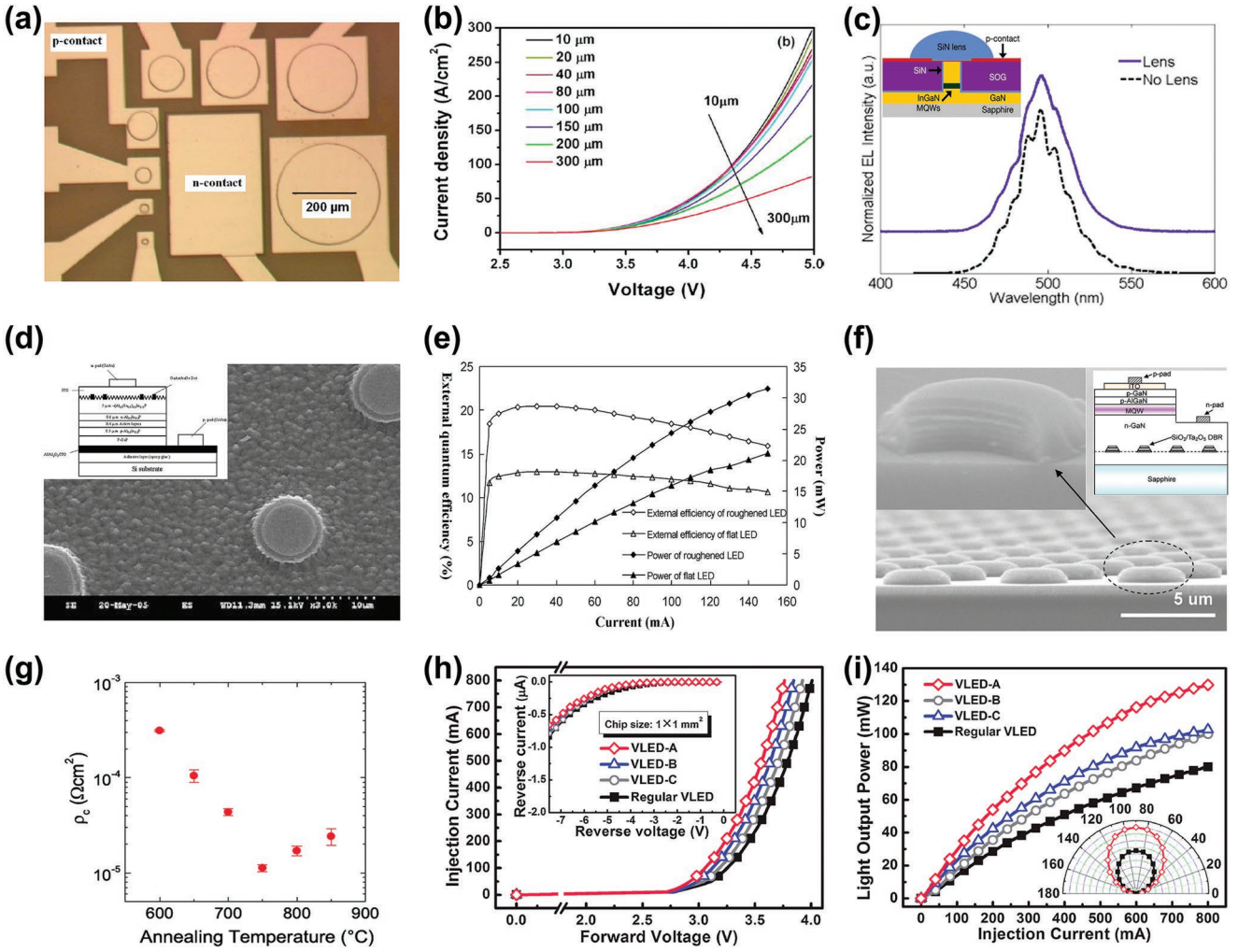

Figure 7. a) Magnified microscope image of the 8 different-sized μLEDs (chip size of 10 × 10 to 300 × 300 μm²). b) *J–V* curves of various-sized μLEDs. Reproduced with permission.[115] Copyright 2010, AIP Publishing. c) Normalized electroluminescence (EL) spectra of μLEDs with and without nanolens. The inset is a schematic illustration of a μLED with a parabolic nanolens. Reproduced with permission.[116] Copyright 2018, IOP Publishing. d) SEM image of surface-roughened AlGaInP μLED. The inset image is a cross-sectional illustration of μLED with n-AlGaInP surface roughening. e) External quantum efficiency and light output power of surface-roughened μLEDs and conventional flat surface μLEDs. Reproduced with permission.[117] Copyright 2005, IEEE. f) SEM image of a patterned reflective layer on GaN μLEDs. The inset image is a cross-sectional illustration of μLEDs with light reflective layer. Reproduced with permission.[118] Copyright 2011, IEEE. g) Contact resistance between n-GaN and Ti/Al/Ni/Au metal layers after annealing process. Reproduced with permission.[119] Copyright 2016, Elsevier. h) *I–V* plots of the various VLEDs (VLED-A: surface-patterned VLED with current spreading layer, VLED-B: surface-patterned VLED, VLED-C: VLED with current spreading layer, Regular VLED: VLED without any additional process). i) Light output power of various VLEDs as a function of injection current. The inset exhibits light angular distribution of VLED-A and regular VLED. Reproduced with permission.[120] Copyright 2011, IOP Publishing.

mother RGB III–V wafers to a display substrate using a patterned PDMS stamp, and interconnected by metal electrode lines. Figure 9c exhibits a full-color PMILED display with a 2190 cd m^{-2} luminance and 127 PPI resolution, enabling uniform μLED transfer yields of 99.7%, 99.5%, and 99.7% in red, green, and blue pixels, respectively.[10] The SEM image in Figure 9d presents a 44 × 44 active-matrix μLED (AMILED) display integrated with microintegrated circuits (μICs). One AMILED pixel was composed of six μLEDs (two red, two green, and two blue LEDs), two μICs and metal electrodes. For μLED operation, a one-bit signal was stored in the μICs composed of 206 complementary metal-oxide-semiconductor-processed transistors in a 38 × 33 μm² area. Figure 9e shows that a high-resolution PMILED display with 1700 PPI was fabricated by flip-chip bonding process.[75] Indium bumps were patterned on the μLED contact pads, interconnecting the 50 000 LED chips to the IC display driver via heat and pressure.

Wearable displays have attracted huge attentions as a visual info-communication tool in the hyperconnected IoT era, due to its hands-free, portable, and lightweight properties. A wearable μLED (WμLED) was realized by transparent elastomeric adhesive (TEA)-based transfer technology using the customized transfer equipment, as displayed in Figure 9f.[129] TEA-based bonding/transfer was optimized by theoretical and experimental analyses for outstanding thermal and humid stability of WμLEDs at 85 °C and 85% relative humidity, as shown in Figure 9g. In

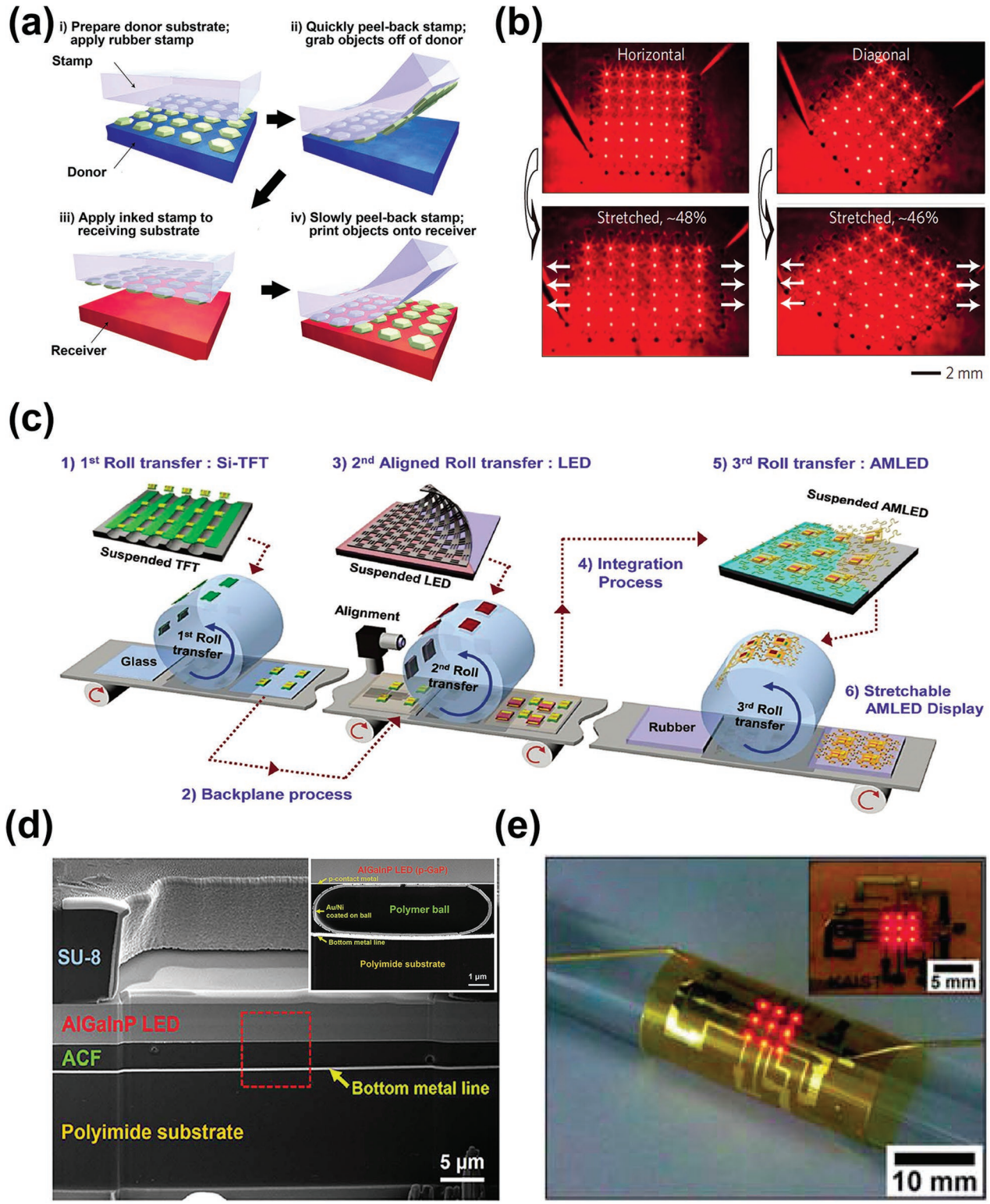

Figure 8. a) Schematic illustrations of μLED printing process using elastomer stamp. Reproduced with permission.[48] Copyright 2006, Springer Nature. b) Photographs of 6 × 6 μLED array, transferred by elastomer stamp-based printing method. Transferred μLEDs maintained their red light under horizontal and diagonal stretching conditions. Reproduced with permission.[121] Copyright 2010, Springer Nature. c) Schematic of roll-based μLED transfer process for stretchable active matrix (AM) display. Reproduced with permission.[122] Copyright 2017, Wiley-VCH. d) Cross-sectional SEM image of ACF-bonded f-VLED. The inset image shows a deformed conductive polymer ball in ACF after compression process. Reproduced with permission.[61] Copyright 2018, Elsevier. e) Self-powered fully-flexible μLED array, composed of f-VLEDs and thin-film nanogenerator on plastic substrate. Reproduced with permission.[60] Copyright 2014, Royal Society of Chemistry.

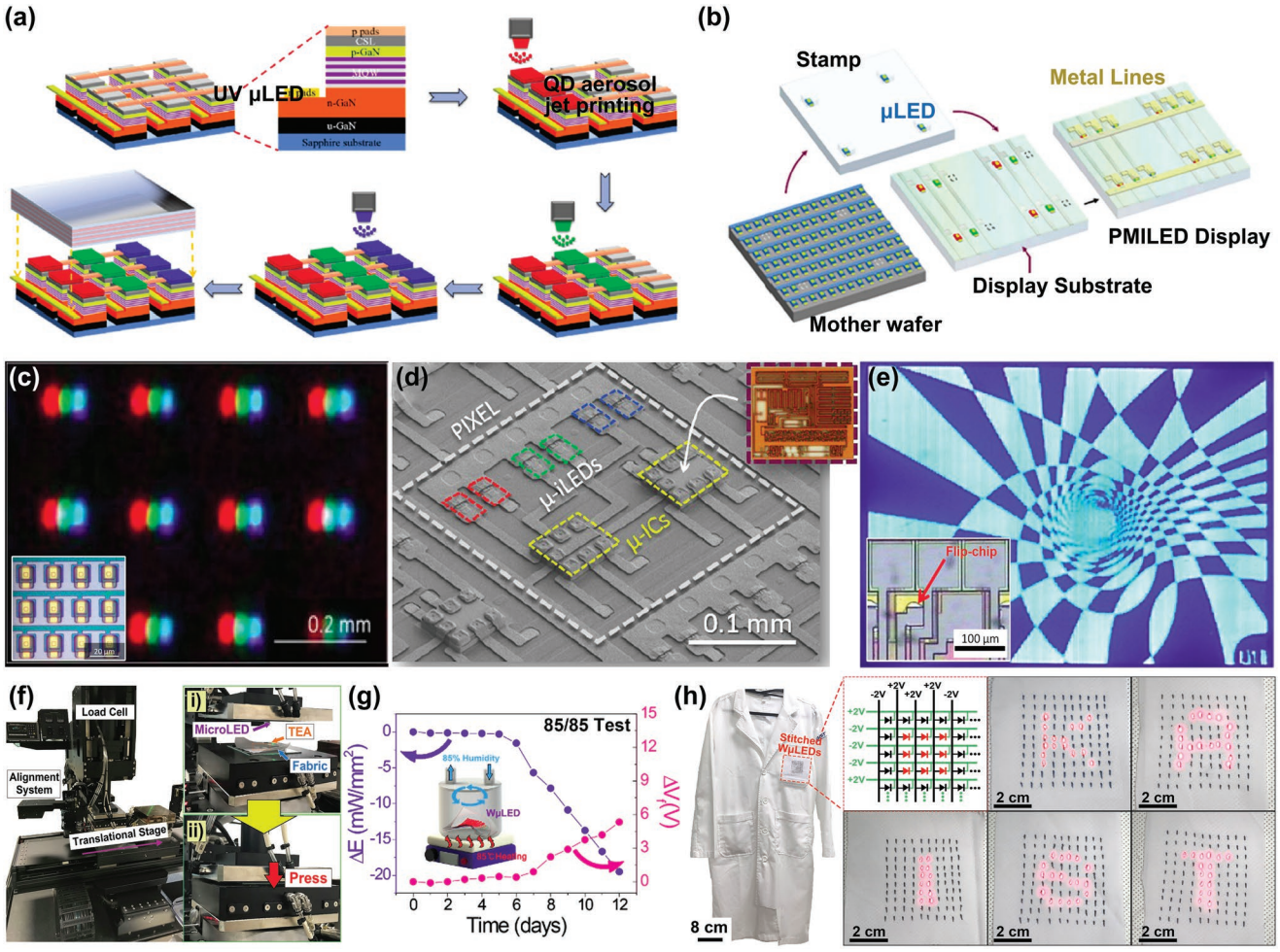

Figure 9. a) Schematic illustration of quantum dot (QD) based full-color μLED display fabrication. Reproduced with permission.[126] Copyright 2015, OSA Publishing. b) Schematic illustration of passive-matrix μLED (PMILED) full-color display using stamping transfer method. Reproduced with permission.[127] Copyright 2017, Wiley-VCH. c) Full-color PMILED display on glass substrate. The left inset is a magnified microscope image of μLED pixels in PMILED. The right inset shows a flexible monochromatic PMILED display on a plastic substrate. d) The left SEM image presents a single pixel of an active-matrix μLED (AMILED) display, composed of RGB μLEDs and microintegrated circuits (μICs). The right photograph exhibits operation of full-color AMILED display. Reproduced with permission.[10] Copyright 2017, Wiley-VCH. e) Photograph of a blue PMILED display, fabricated by flip-chip bonding process. The inset image is a magnified microscope image of the bonded μLEDs by indium solder balls. Reproduced with permission.[75] Copyright 2014, IEEE. f) Photograph of the μLED transfer equipment, which can transfer the μLEDs from the rigid mother wafer to a target substrate, such as glass, Si wafers, plastic films, and fabric substrate. g) Harsh environmental testing results of WμLED at 85 °C and 85% relative humidity conditions. The inset image shows WμLEDs, operating in a chemical detergent solution. h) 10 × 10 wearable PMILED display, emitting red light to produce letters K, A, I, S, and T. Reproduced with permission.[129] Copyright 2018, Elsevier.

addition, WμLEDs maintained their optical performance in harsh mechanical bending (100 000 cycles of bending/unbending motions) and artificial sunlight conditions (340 mW m^{-2} of light power). Figure 9h presents a PM WμLED display on the pocket of a clothing, operated by a common cathode configuration of a 10 × 10 array. The wearable μLED display stably illuminated the red light on the fabric, demonstrating letters of K, A, I, S, and T. It is noteworthy that μLEDs are suitable for not only wearable displays, but also for human–interface applications.

4.2. Biomedical Applications

Flexible μLEDs have been widely utilized in biomedical applications, including biosensors, healthcare devices, and optogenetic stimulators, due to its outstanding biocompatibility, low heating property, and excellent stability.[12,14,23,24,49,61,130–133] Optogenetics is a promising cortical mapping technology, in which the microsized neural cells are stimulated using visible light for behavior control.[107,134] Low heat from a photostimulator is essential to minimize brain tissue damage in optogenetic applications. In this perspective, flexible vertical μLEDs have been exploited as an optogenetic stimulator in complex animal behavior due to their low thermal damage and conformal insertion. **Figure 10** shows examples of flexible biomedical devices using thin-film μLEDs. Figure 10a displays a photograph of an f-VLED optical module inserted under a mouse skull through a small cranial slit.[107] High-performance red f-VLEDs with optical power density of 25 mW mm^{-2} wrapped the corrugated and curved mouse

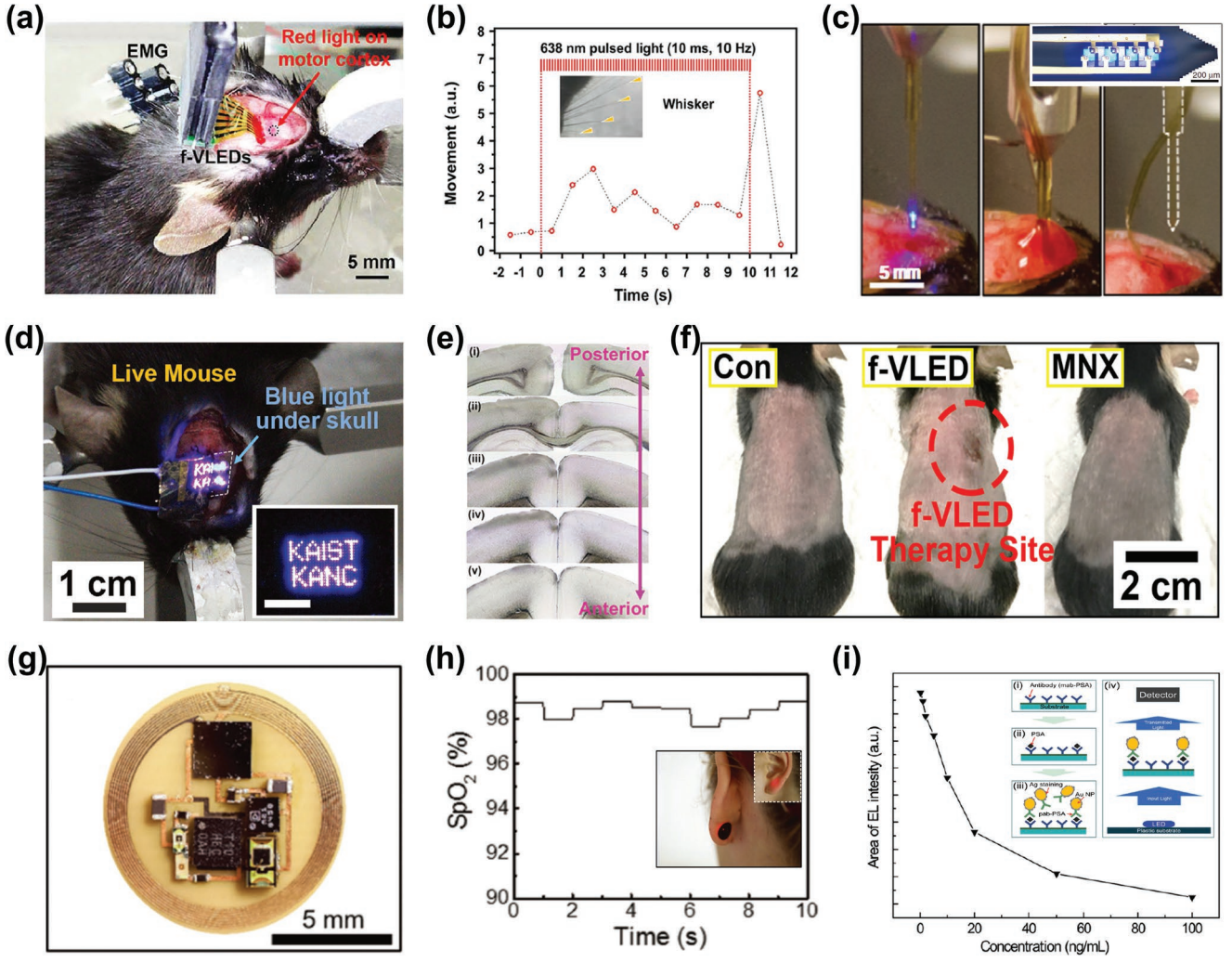

Figure 10. a) Photograph of red f-VLED array, stimulating mouse motor cortex on brain surface. b) Mouse whisker movements as a function of stimulating time. Mouse whiskers are indicated by yellow arrow in the inset image. Reproduced with permission.[61] Copyright 2018, Elsevier. c) Insertion and removal process of injectable optogenetic device, composed of electrodes, GaN μLEDs, photodiodes, and temperature sensors. Reproduced with permission.[12] Copyright 2013, AAAS. d) 30 × 30 PMILED array on mouse brain surface, displaying the word "KAIST-KANC." e) Cross-sectional segments of mouse brain after light irradiation and subtraction of optoelectronic device. Reproduced with permission.[23] Copyright 2018, Wiley-VCH. f) Mouse dorsal skin images after hair-growth treatment, showing negative control group (left), minoxidil-treated group (right), and f-VLED-treated group (center). Reproduced with permission.[49] Copyright 2018, American Chemical Society. g) Photograph of wearable pulse oximeter device, composed of μLEDs, photodiodes, and flexible antennas. h) SpO2 signal from back of earlobe as a function of measurement time. The inset image exhibits an attached pulse oximetry device on earlobe. Reproduced with permission.[14] Copyright 2016, Wiley-VCH. i) Concentration analysis of prostate-specific antigen (PSA) using μLED-based flexible biosensor. The inset presents schematic procedure of PSA sensing mechanism. Reproduced with permission.[132] Copyright 2011, Elsevier.

brain, and photostimulated the red-shifted channelrhodopsin (chrimson) to modulate mouse whisker and forelimb movements. As shown in Figure 10b, the movements of the living mouse whiskers were controlled by pulsed red light during 10 s of illumination without any side-effects. Figure 10c exhibits GaN μLED-based injectable needles for stimulation of the mouse deep brain.[12] The implantable photostimulator was operated to optogenetically control the mouse brain, collecting neuronal signals and temperature changes simultaneously. As presented in Figure 10d, ultrathin f-VLEDs with thickness of 15 μm were fabricated by a laser lift-off and simple monolithic LED process, and inserted under the mouse skull to wirelessly illuminate the cerebral cortex with blue light.[23] The 30 × 30 f-VLED arrays exhibited outstanding optical power density of 30 mW mm^{-2}, long lifespan of ≈12 years, and superior mechanical durability in harsh bending states. After photostimulation and extraction of f-VLEDs, the mouse brain showed neither mechanical nor thermal damage in the histological analysis, as shown in Figure 10e.

Several researchers have developed flexible μLED-based healthcare devices to treat chronic skin diseases, and measure biological signals (e.g., SpO_2, heart beating rate, and antigen-antibody reaction). Lee et al. demonstrated wearable trichogenic photostimulators using high-performance red f-VLEDs

with an irradiance of ≈30 mW mm^{-2}.[49] Wearable f-VLEDs presented a skin phototherapic suitability such as low heat generation, ultrathin thickness of 20 μm, and remarkable mechanical reliability during 100 000 bending/unbending motions. As shown in Figure 10f, mouse dorsal skin, which was phototreated by red f-VLEDs, exhibited more hair follicles and faster hair regrowth than those of other control groups. Superior hair-growth effects of red f-VLED was attributed to the deep skin penetration of red light to 1–2 mm below the mouse skin, locating most of hair follicles. Figure 10g represents the battery-free wearable pulse oximetry device with wireless power transmission system, composed of a red μLED, an infrared (IR) μLED, photodiode (PD), and flexible antennas.[14] The wearable pulse oximetry device detected blood oxygen saturation (SpO_2) and extracted heart rate on a human earlobe by analyzing the PD response associated with LED signals, as shown in Figure 10h. Figure 10i presents a prostate-specific antigen (PSA) biosensor using water-resistant flexible GaN μLEDs on a liquid crystal polymer.[132] The flexible GaN μLEDs detected the PSA concentration based on light intensity differences before and after antigen–antibody reactions.

5. Conclusion

This review paper has described an overview of μLEDs for next-generation displays and flexible biomedical devices.[135,136] Implementation of high-performance μLEDs have led to a wide range of technical advances in the fields of μLED device structures, performance enhancement, transfer processes, and packaging methods. Optimum performance enhancements of μLEDs were achieved by using vertical structure, small chip size, lens integration, surface treatment, reflectors, and current spreading layers. PM and AM μLED displays were achieved using transfer methods of electrostatic transfer, elastomer stamping, laser-assisted transfer, electromagnetic transfer, and pressure-based transfer. For biomedical applications, flexible optogenetic and trichogenic photostimulators were demonstrated using ACF-based fully packaged thin-film μLED technologies or a simple monolithic fabrication method. The μLEDs are expected to open new paradigm shifts for future optoelectronic systems in the upcoming IoT and healthcare era.[137,138]

Acknowledgements

H.E.L., J.H.S., and J.H.P. contributed equally to this work. This work was financially supported by Nano Material Technology Development Program (Grant No. 2016M3A7B4910636), and Creative Materials Discovery Program (Grant No. NRF-2016M3D1A1900035) through the National Research Foundation of Korea (NRF) funded by the Ministry of Science, ICT and Future Planning (MSIP). This work was supported by National Research Foundation (NRF) of Korea and funded by the Ministry of Science, ICT, and Future Planning (Grant No. NRF-2017R1A2A1A18071765).

Conflict of Interest

The authors declare no conflict of interest.

Keywords

biomedical applications, device transfer processes, microLED displays, microLEDs, wearable applications

Received: November 14, 2018
Revised: January 13, 2019
Published online: April 3, 2019

[1] L. Zhang, F. Ou, W. C. Chong, Y. Chen, Y. Zhu, Q. Li, *SID Symp. Dig. Tech. Pap.* **2018**, *49*, 786.
[2] K. Parikh, K. Ahmed, N. Matsumura, D. Gottardo, R. Cancel, B. Girvin, R. Woodbeck, *SID Symp. Dig. Tech. Pap.* **2016**, *47*, 570.
[3] E. F. Schubert, J. K. Kim, *Science* **2005**, *308*, 1274.
[4] Y.-T. Liu, K.-Y. Liao, C.-L. Lin, Y.-L. Li, *SID Symp. Dig. Tech. Pap.* **2018**, *49*, 874.
[5] J. Yoon, S.-M. Lee, D. Kang, M. A. Meitl, C. A. Bower, J. A. Rogers, *Adv. Opt. Mater.* **2015**, *3*, 1313.
[6] D. A. Gaul, W. S. Rees Jr., *Adv. Mater.* **2000**, *12*, 935.
[7] G. Chen, M. Craven, A. Kim, A. Munkholm, S. Watanabe, M. Camras, W. Götz, F. Steranka, *Phys. Status Solidi A* **2008**, *205*, 1086.
[8] R. Meerheim, S. Scholz, S. Olthof, G. Schwartz, S. Reineke, K. Walzer, K. Leo, *J. Appl. Phys.* **2008**, *104*, 014510.
[9] J. Day, J. Li, D. Y. C. Lie, C. Bradford, J. Y. Lin, H. X. Jiang, *Appl. Phys. Lett.* **2011**, *99*, 031116.
[10] R. S. Cok, M. Meitl, R. Rotzoll, G. Melnik, A. Fecioru, A. J. Trindade, B. Raymond, S. Bonafede, D. Gomez, T. Moore, C. Prevatte, E. Radauscher, S. Goodwin, P. Hines, C. A. Bower, *J. Soc. Inf. Disp.* **2017**, *25*, 589.
[11] S. J. Phenix, *SID Symp. Dig. Tech. Pap.* **2017**, *48*, 608.
[12] T.-I. Kim, J. G. McCall, Y. H. Jung, X. Huang, E. R. Siuda, Y. Li, J. Song, Y. M. Song, H. A. Pao, R.-H. Kim, C. Lu, S. D. Lee, I.-S. Song, G. Shin, R. Al-Hasani, S. Kim, M. P. Tan, Y. Huang, F. G. Omenetto, J. A. Rogers, M. R. Bruchas, *Science* **2013**, *340*, 211.
[13] C.-M. Kang, J.-Y. Lee, M.-D. Park, S.-H. Mun, S.-Y. Choi, K. Kim, S. Kim, J.-P. Shim, D.-S. Lee, *SID Symp. Dig. Tech. Pap.* **2018**, *49*, 604.
[14] J. Kim, P. Gutruf, A. M. Chiarelli, S. Y. Heo, K. Cho, Z. Xie, A. Banks, S. Han, K.-I. Jang, J. W. Lee, K.-T. Lee, X. Feng, Y. Huang, M. Fabiani, G. Gratton, U. Paik, J. A. Rogers, *Adv. Funct. Mater.* **2017**, *27*, 1604373.
[15] H. Qiu, W. Lu, S. Zhang, H. Jiao, *SID Symp. Dig. Tech. Pap.* **2018**, *49*, 1399.
[16] T. Wu, C.-W. Sher, Y. Lin, C.-F. Lee, S. Liang, Y. Lu, S.-W. Huang Chen, W. Guo, H.-C. Kuo, Z. Chen, *Appl. Sci.* **2018**, *8*, 1557.
[17] R.-H. Horng, H.-Y. Chien, F.-G. Tarntair, D.-S. Wuu, *IEEE J. Electron Devices Soc.* **2018**, *6*, 1064.
[18] A. Daami, F. Olivier, L. Dupré, F. Henry, F. Templier, *SID Symp. Dig. Tech. Pap.* **2018**, *49*, 790.
[19] J. H. Park, J. Seo, C. Kim, D. J. Joe, H. E. Lee, T. H. Im, J. Y. Seok, C. K. Jeong, B. S. Ma, H. K. Park, T.-S. Kim, K. J. Lee, *Adv. Sci.* **2018**, *5*, 1801146.
[20] G. J. Woodgate, J. Harrold, *SID Symp. Dig. Tech. Pap.* **2018**, *49*, 1559.
[21] C.-M. Kang, S.-J. Kang, S.-H. Mun, S.-Y. Choi, J.-H. Min, S. Kim, J.-P. Shim, D.-S. Lee, *Sci. Rep.* **2017**, *7*, 10333.
[22] V. R. Marinov, *SID Symp. Dig. Tech. Pap.* **2018**, *49*, 692.
[23] H. E. Lee, J. Choi, S. H. Lee, M. Jeong, J. H. Shin, D. J. Joe, D. Kim, C. W. Kim, J. H. Park, J. H. Lee, D. Kim, C.-S. Shin, K. J. Lee, *Adv. Mater.* **2018**, *30*, 1800649.
[24] J. Kim, G. A. Salvatore, H. Araki, A. M. Chiarelli, Z. Xie, A. Banks, X. Sheng, Y. Liu, J. W. Lee, K.-I. Jang, S. Y. Heo, K. Cho, H. Luo, B. Zimmerman, J. Kim, L. Yan, X. Feng, S. Xu, M. Fabiani, G. Gratton, Y. Huang, U. Paik, J. A. Rogers, *Sci. Adv.* **2016**, *2*, e1600418.

[25] Y. Chen, J. Au, P. Kazlas, A. Ritenour, H. Gates, M. McCreary, *Nature* **2003**, *423*, 136.
[26] S. Il Park, G. Shin, J. G. McCall, R. Al-Hasani, A. Norris, L. Xia, D. S. Brenner, K. N. Noh, S. Y. Bang, D. L. Bhatti, K.-I. Jang, S.-K. Kang, A. D. Mickle, G. Dussor, T. J. Price, R. W. Gereau, M. R. Bruchas, J. A. Rogers, *Proc. Natl. Acad. Sci. USA* **2016**, *113*, E8169.
[27] D. S. Hermann, *2018 25th Int. Workshop on Active-Matrix Flatpanel Displays and Devices (AM-FPD)* **2018**, 1.
[28] R.-H. Horng, H.-Y. Chien, K.-Y. Chen, W.-Y. Tseng, Y.-T. Tsai, F.-G. Tarntair, *IEEE J. Electron Devices Soc.* **2018**, *6*, 475.
[29] Z. Deng, B. Zheng, J. Zheng, L. Wu, W. Yang, Z. Lin, P. Shen, J. Li, *SID Symp. Dig. Tech. Pap.* **2018**, *49*, 996.
[30] H.-W. Chen, J.-H. Lee, B.-Y. Lin, S. Chen, S.-T. Wu, *Light: Sci. Appl.* **2018**, *7*, 17168.
[31] F. J. Henley, *SID Symp. Dig. Tech. Pap.* **2018**, *49*, 688.
[32] G. Tan, Y. Huang, M.-C. Li, S.-L. Lee, S.-T. Wu, *Opt. Express* **2018**, *26*, 16572.
[33] C.-M. Kang, J.-Y. Lee, D.-J. Kong, J.-P. Shim, S. Kim, S.-H. Mun, S.-Y. Choi, M.-D. Park, J. Kim, D.-S. Lee, *ACS Photonics* **2018**, *5*, 4413.
[34] E. H. Virey, N. Baron, *SID Symp. Dig. Tech. Pap.* **2018**, *49*, 593.
[35] C. Prevatte, E. Radauscher, M. A. Meitl, D. Gomez, K. Ghosal, S. Bonafede, B. Raymond, T. Moore, A. J. Trindade, P. Hines, C. A. Bower, *2017 IEEE 67th Electronic Components and Technology Conf. (ECTC)* **2017**, 1098.
[36] R. Chaji, E. Fathi, A. Zamani, *SID Symp. Dig. Tech. Pap.* **2017**, *48*, 264.
[37] C.-C. Lin, Y.-H. Fang, M.-J. Kao, P.-K. Huang, F.-P. Chang, L.-C. Yang, C.-I. Wu, *SID Symp. Dig. Tech. Pap.* **2018**, *49*, 782.
[38] T.-I. Kim, Y. H. Jung, J. Song, D. Kim, Y. Li, H.-S Kim, I.-S. Song, J. J. Wierer, H. A. Pao, Y. Huang, J. A. Rogers, *Small* **2012**, *8*, 1643.
[39] K. J. Lee, M. J. Motala, M. A. Meitl, W. R. Childs, E. Menard, A. K. Shim, J. A. Rogers, R. G. Nuzzo, *Adv. Mater.* **2005**, *17*, 2332.
[40] M.-H. Wu, Y.-H. Fang, C.-H. Chao, (Industrial Technology Research Institute), *US Patent 0172253 A1*, **2016**.
[41] H.-s. Kim, E. Brueckner, J. Song, Y. Li, S. Kim, C. Lu, J. Sulkin, K. Choquette, Y. Huang, R. G. Nuzzo, J. A. Rogers, *Proc. Natl. Acad. Sci. USA* **2011**, *108*, 10072.
[42] R.-H. Kim, M.-H. Bae, D. G. Kim, H. Cheng, B. H. Kim, D.-H. Kim, M. Li, J. Wu, F. Du, H.-S. Kim, S. Kim, D. Estrada, S. W. Hong, Y. Huang, E. Pop, J. A. Rogers, *Nano Lett.* **2011**, *11*, 3881.
[43] J. A. Rogers, P. M. Ferreira, R. Saeidpourazar, *US Patent 0036928 A1*, **2013**.
[44] R.-H. Kim, S. Kim, Y. M. Song, H. Jeong, T.-I. Kim, J. Lee, X. Li, K. D. Choquette, J. A. Rogers, *Small* **2012**, *8*, 3123.
[45] A. Bibl, J. A. Higginson, H.-F. S. Law, H.-H. Hu (LuxVue Technology Corporation), *US Patent 0299837 A1*, **2014**.
[46] R. Saeidpourazar, M. D. Sangid, J. A. Rogers, P. M. Ferreira, *J. Manuf. Processes* **2012**, *14*, 416.
[47] N. Ahmed, A. Carlson, J. A. Rogers, P. M. Ferreira, *J. Manuf. Processes* **2012**, *14*, 90.
[48] M. A. Meitl, Z.-T. Zhu, V. Kumar, K. J. Lee, X. Feng, Y. Y. Huang, I. Adesida, R. G. Nuzzo, J. A. Rogers, *Nat. Mater.* **2006**, *5*, 33.
[49] H. E. Lee, S. H. Lee, M. Jeong, J. H. Shin, Y. Ahn, D. Kim, S. H. Oh, S. H. Yun, K. J. Lee, *ACS Nano* **2018**, *12*, 9587.
[50] C.-K. Li, Y.-R. Wu, *IEEE Trans. Electron Devices* **2012**, *59*, 400.
[51] D. Feezell, S. Nakamura, *C. R. Phys.* **2018**, *19*, 113.
[52] S. Nakamura, M. R. Krames, *Proc. IEEE* **2013**, *101*, 2211.
[53] C. Griffin, H. X. Zhang, B. Guilhabert, D. Massoubre, E. Gu, M. D. Dawson, *2007 Conf. on Lasers and Electro-Optics (CLEO)* **2007**, 1.
[54] F. K. Yam, Z. Hassan, *Microelectron. J.* **2005**, *36*, 129.
[55] J. J. Wierer, D. A. Steigerwald, M. R. Krames, J. J. O'Shea, M. J. Ludowise, G. Christenson, Y.-C. Shen, C. Lowery, P. S. Martin, S. Subramanya, W. Götz, N. F. Gardner, R. S. Kern, S. A. Stockman, *Appl. Phys. Lett.* **2001**, *78*, 3379.
[56] O. B. Shchekin, J. E. Epler, T. A. Trottier, T. Margalith, D. A. Steigerwald, M. O. Holcomb, P. S. Martin, M. R. Krames, *Appl. Phys. Lett.* **2006**, *89*, 071109.
[57] X. A. Cao, S. D. Arthur, *Appl. Phys. Lett.* **2004**, *85*, 3971.
[58] P. Tian, J. J. D. McKendry, Z. Gong, S. Zhang, S. Watson, D. Zhu, I. M. Watson, E. Gu, A. E. Kelly, C. J. Humphreys, M. D. Dawson, *J. Appl. Phys.* **2014**, *115*, 033112.
[59] K. Bao, X. N. Kang, B. Zhang, T. Dai, Y. J. Sun, Q. Fu, G. J. Lian, G. C. Xiong, G. Y. Zhang, Y. Chen, *Appl. Phys. Lett.* **2008**, *92*, 141104.
[60] C. K. Jeong, K.-I. Park, J. H. Son, G.-T. Hwang, S. H. Lee, D. Y. Park, H. E. Lee, H. K. Lee, M. Byun, K. J. Lee, *Energy Environ. Sci.* **2014**, *7*, 4035.
[61] S. H. Lee, J. Kim, J. H. Shin, H. E. Lee, I.-S. Kang, K. Gwak, D.-S. Kim, D. Kim, K. J. Lee, *Nano Energy* **2018**, *44*, 4.
[62] B. K. You, J. M. Kim, D. J. Joe, K. Yang, Y. Shin, Y. S. Jung, K. J. Lee, *ACS Nano* **2016**, *10*, 9478.
[63] W. Christiaens, E. Bosman, J. Vanfleteren, *IEEE Trans. Compon. Packag. Technol.* **2010**, *33*, 754.
[64] K.-L. Suk, H.-Y. Son, C.-K. Chung, J. D. Kim, J.-W. Lee, K.-W. Paik, *Microelectron. Reliab.* **2012**, *52*, 225.
[65] B. K. You, W. I. Park, J. M. Kim, K. Park, H. K. Seo, J. Y. Lee, Y. S. Jung, K. J. Lee, *ACS Nano* **2014**, *8*, 9492.
[66] H. E. Lee, J. H. Park, T. J. Kim, D. Im, J. H. Shin, D. H. Kim, B. Mohammad, I.-S. Kang, K. J. Lee, *Adv. Funct. Mater.* **2018**, *28*, 1801690.
[67] L. Zhang, F. Ou, W. C. Chong, Y. Chen, Q. Li, *J. Soc. Inf. Disp.* **2018**, *26*, 137.
[68] S. Kim, H. Y. Jeong, S. K. Kim, S.-Y. Choi, K. J. Lee, *Nano Lett.* **2011**, *11*, 5438.
[69] W. I. Park, B. K. You, B. H. Mun, H. K. Seo, J. Y. Lee, S. Hosaka, Y. Yin, C. a. Ross, K. J. Lee, Y. S. Jung, *ACS Nano* **2013**, *7*, 2651.
[70] D. Peng, K. Zhang, Z. Liu, *IEEE J. Electron Devices Soc.* **2017**, *5*, 90.
[71] D. Peng, K. Zhang, V. S.-D. Chao, W. Mo, K. M. Lau, Z. Liu, *J. Disp. Technol.* **2016**, *12*, 742.
[72] C.-C. An, M.-H. Wu, Y. Huang, T.-H. Chen, C.-H. Chao, W.-Y. Yeh, *2011 6th Int. Microsystems, Packaging, Assembly and Circuits Technology Conf. (IMPACT)* **2011**, 336.
[73] J. Herrnsdorf, J. J. D. McKendry, S. Zhang, E. Xie, R. Ferreira, D. Massoubre, A. M. Zuhdi, R. K. Henderson, I. Underwood, S. Watson, A. E. Kelly, E. Gu, M. D. Dawson, *IEEE Trans. Electron Devices* **2015**, *62*, 1918.
[74] K. Zhang, D. Peng, W. C. Chong, K. M. Lau, Z. Liu, *IEEE Trans. Electron Devices* **2016**, *63*, 4832.
[75] W. C. Chong, W. K. Cho, Z. J. Liu, C. H. Wang, K. M. Lau, *2014 IEEE Compound Semiconductor Integrated Circuit Symp. (CSICS)* **2014**, 1.
[76] X. Li, L. Wu, Z. Liu, B. Hussain, W. C. Chong, K. M. Lau, C. P. Yue, *J. Lightwave Technol.* **2016**, *34*, 3449.
[77] J. Herrnsdorf, J. J. D. McKendry, E. Xie, M. J. Strain, I. M. Watson, E. Gu, M. D. Dawson, *2016 IEEE Photonics Society Summer Topical Meeting Series (SUM)* **2016**, 173.
[78] F. Templier, L. Dupré, B. Dupont, A. Daami, B. Aventurier, F. Henry, D. Sarrasin, S. Renet, F. Berger, F. Olivier, L. Mathieu, in *Proc. SPIE* **2018**, *10556*, 105560l.
[79] F. Templier, *J. Soc. Inf. Disp.* **2016**, *24*, 669.
[80] E. Xie, M. Stonehouse, R. Ferreira, J. J. D. McKendry, J. Herrnsdorf, X. He, S. Rajbhandari, H. Chun, A. V. N. Jalajakumari, O. Almer, G. Faulkner, I. M. Watson, E. Gu, R. Henderson, D. O'Brien, M. D. Dawson, *IEEE Photonics J.* **2017**, *9*, 1.
[81] M. Ogihara, H. Fujiwara, M. Mutoh, T. Suzuki, T. Igari, T. Sagimori, H. Kurokawa, T. Kaneto, H. Furuta, I. Abiko, M. Sakuta, *Electron. Lett.* **2006**, *42*, 881.

[82] C. C. Dong, F. Yu, T. Bao, W. Zhang, F. Dai, D. Yang, *2018 9th Int. Conf. on Electronic Packaging Technology (ICEPT)* **2018**, 652.
[83] D. H. Kim, H. G. Yoo, D. J. Joe, K. J. Lee, *2015 IEEE Int. Electron Devices Meet. (IEDM)* **2015**, 19.3.1.
[84] D. H. Kim, H. G. Yoo, S. M. Hong, B. Jang, D. Y. Park, D. J. Joe, J.-H. Kim, K. J. Lee, *Adv. Mater.* **2016**, *28*, 8371.
[85] J. H. Han, K. M. Bae, S. K. Hong, H. Park, J.-H. Kwak, H. S. Wang, D. J. Joe, J. H. Park, Y. H. Jung, S. Hur, C. D. Yoo, K. J. Lee, *Nano Energy* **2018**, *53*, 658.
[86] J. H. Han, J.-H. Kwak, D. J. Joe, S. K. Hong, H. S. Wang, J. H. Park, S. Hur, K. J. Lee, *Nano Energy* **2018**, *53*, 198.
[87] D. Y. Park, D. J. Joe, D. H. Kim, H. Park, J. H. Han, C. K. Jeong, H. Park, J. G. Park, B. Joung, K. J. Lee, *Adv. Mater.* **2017**, *29*, 1702308.
[88] H. S. Lee, J. Chung, G.-T. Hwang, C. K. Jeong, Y. Jung, J.-H. Kwak, H. Kang, M. Byun, W. D. Kim, S. Hur, S.-H. Oh, K. J. Lee, *Adv. Funct. Mater.* **2014**, *24*, 6914.
[89] A. Khan, K. Balakrishnan, T. Katona, *Nat. Photonics* **2008**, *2*, 77.
[90] L. Shi, A. K. Srivastava, A. Cheung, C.-T. Hsieh, C.-L. Hung, C.-H. Lin, C. Lin, N. Sugiura, C.-W. Kuo, V. G. Chigrinov, H. S. Kwok, *J. Soc. Inf. Disp.* **2018**, *26*, 325.
[91] D.-U. Jin, J.-S. Lee, T.-W. Kim, S. An, D. Straykhilev, Y.-S. Pyo, H.-S. Kim, D.-B. Lee, Y.-G. Mo, H.-D. Kim, H.-K. Chung, *SID Symp. Dig. Tech. Pap.* **2009**, *40*, 983.
[92] J.-K. Yoon, E.-M. Park, J.-S. Son, H.-W. Shin, H.-E. Kim, M. Yee, H.-G. Kim, C.-H. Oh, B.-C. Ahn, *SID Symp. Dig. Tech. Pap.* **2013**, *44*, 326.
[93] J. M. M. Santos, B. E. Jones, P. J. Schlosser, S. Watson, J. Herrnsdorf, B. Guilhabert, J. J. D. McKendry, J. De Jesus, T. A. Garcia, M. C. Tamargo, A. E. Kelly, J. E. Hastie, N. Laurand, M. D. Dawson, *Semicond. Sci. Technol.* **2015**, *30*, 035012.
[94] W. Henry, C. Percival, *SID Symp. Dig. Tech. Pap.* **2016**, *47*, 747.
[95] R. Asaki, S. Yokoyama, H. Kitagawa, S. Makimura, F. Abe, T. Yamazaki, T. Kato, M. Kanno, Y. Onoyama, E. Hasegawa, K. Uchino, *SID Symp. Dig. Tech. Pap.* **2014**, *45*, 219.
[96] F. Ou, W. C. Chong, Q. Xu, Y. Chen, Q. Li, L. Zhang, *SID Symp. Dig. Tech. Pap.* **2018**, *49*, 1677.
[97] R. G. Nuzzo, J. A. Rogers, E. Menard, K. J. Lee, D.-Y. Khang, Y. Sun, M. Meitl, Z. Zhu,F. OuW. C. Chong, Q. Xu, Y. Chen, Q. Li, (University of Illinois), *US Patent 8,664,699 B2*, **2015**.
[98] J. A. Rogers, R. Nuzzo, H.-S. Kim, E. Brueckner, S. I. Park, R. H. Kim, (University of Illinois), *US Patent 2015/0132873 A1*, **2015**.
[99] K. J. Lee, S. H. Lee, J. H. Son, (Korea Advanced Institute of Science and Technology), *KR. 10–1362516*, **2014**.
[100] K. J. Lee, S. H. Lee, H. E. Lee, (Korea Advanced Institute of Science and Technology), *KR. 10–1718652*, **2017**.
[101] H. Zhang, J. A. Rogers, *Adv. Opt. Mater.* **2018**, *1800936*, 1800936.
[102] A. Bibl, J. A. Higginson, H.-F. S. Law, H.-H. Hu, (LuxVue Technology Corporation), *US Patent 8349116 B1*, **2013**.
[103] A. Bibl, J. A. Higginson, H.-F. S. Law, H.-H. Hu, (LuxVue Technology Corporation), *US Patent 8333860 B1*, **2012**.
[104] V. R. Marinov, O. Swenson, Y. Atanasov, N. Schneck, *Microelectron. Eng.* **2013**, *101*, 23.
[105] V. Marinov, O. Swenson, R. Miller, F. Sarwar, Y. Atanasov, M. Semler, S. Datta, *IEEE Trans. Compon., Packag., Manuf. Technol.* **2012**, *2*, 569.
[106] R. Miller, V. Marinov, O. Swenson, Z. Chen, M. Semler, *IEEE Trans. Compon., Packag., Manuf. Technol.* **2012**, *2*, 971.
[107] S. H. Lee, J. Kim, J. H. Shin, H. E. Lee, I.-S. Kang, K. Gwak, D.-S. Kim, D. Kim, K. J. Lee, *Nano Energy* **2018**, *44*, 447.
[108] H. G. Yoo, M. Byun, C. K. Jeong, K. J. Lee, *Adv. Mater.* **2015**, *27*, 3982.
[109] B. H. Mun, B. K. You, S. R. Yang, H. G. Yoo, J. M. Kim, W. I. Park, Y. Yin, M. Byun, Y. S. Jung, K. J. Lee, *ACS Nano* **2015**, *9*, 4120.
[110] B. K. You, M. Byun, S. Kim, K. J. Lee, *ACS Nano* **2015**, *9*, 6587.
[111] S. Kim, J. H. Son, S. H. Lee, B. K. You, K.-I. Park, H. K. Lee, M. Byun, K. J. Lee, *Adv. Mater.* **2014**, *26*, 7480.
[112] H. G. Yoo, S. Kim, K. J. Lee, *RSC Adv.* **2014**, *4*, 20017.
[113] C.-M. Kang, D.-J. Kong, J.-P. Shim, S. Kim, S.-B. Choi, J.-Y. Lee, J.-H. Min, D.-J. Seo, S.-Y. Choi, D.-S. Lee, *Opt. Express* **2017**, *25*, 2489.
[114] C. Chu, C. Cheng, W. Liu, J. Chu, F. Fan, H. Cheng, T. Doan, C. A. Tran, *Proc. IEEE* **2010**, *98*, 1197.
[115] Z. Gong, S. Jin, Y. Chen, J. McKendry, D. Massoubre, I. M. Watson, E. Gu, M. D. Dawson, *J. Appl. Phys.* **2010**, *107*, 013103.
[116] B. Demory, K. Chung, A. Katcher, J. Sui, H. Deng, P. Ku, *Nanotechnology* **2018**, *29*, 165201.
[117] Y. J. Lee, H. C. Kuo, S. C. Wang, T. C. Hsu, M. H. Hsieh, M. J. Jou, B. J. Lee, *IEEE Photonics Technol. Lett.* **2005**, *17*, 2289.
[118] W.-L. Lin, D.-S. Wuu, S.-C. Huang, R.-H. Horng, *IEEE Trans. Electron Devices* **2011**, *58*, 173.
[119] G. Greco, F. Iucolano, F. Roccaforte, *Appl. Surf. Sci.* **2016**, *383*, 324.
[120] W.-C. Lee, S.-J. Wang, P.-R. Wang, K.-M. Uang, T.-M. Chen, D.-M. Kuo, P.-H. Wang, *Appl. Phys. Express* **2011**, *4*, 072104.
[121] R.-H. Kim, D.-H. Kim, J. Xiao, B. H. Kim, S.-I. Park, B. Panilaitis, R. Ghaffari, J. Yao, M. Li, Z. Liu, V. Malyarchuk, D. G. Kim, A.-P. Le, R. G. Nuzzo, D. L. Kaplan, F. G. Omenetto, Y. Huang, Z. Kang, J. A. Rogers, *Nat. Mater.* **2010**, *9*, 929.
[122] M. Choi, B. Jang, W. Lee, S. Lee, T. W. Kim, H. Lee, J. Kim, J. Ahn, *Adv. Funct. Mater.* **2017**, *27*, 1606005.
[123] G.-T. Hwang, V. Annapureddy, J. H. Han, D. J. Joe, C. Baek, D. Y. Park, D. H. Kim, J. H. Park, C. K. Jeong, K.-I. Park, J.-J. Choi, D. K. Kim, J. Ryu, K. J. Lee, *Adv. Energy Mater.* **2016**, *6*, 1.
[124] S. J. Kim, H. E. Lee, H. Choi, Y. Kim, J. H. We, J. S. Shin, K. J. Lee, B. J. Cho, *ACS Nano* **2016**, *10*, 10851.
[125] K.-I. Park, J. H. Son, G.-T. Hwang, C. K. Jeong, J. Ryu, M. Koo, I. Choi, S. H. Lee, M. Byun, Z. L. Wang, K. J. Lee, *Adv. Mater.* **2014**, *26*, 2514.
[126] H. Han, H.-Y. Lin, C. Lin, W. Chong, J. Li, K.-J. Chen, P. Yu, T.-M. Chen, H. Chen, K. Lau, H. Kuo, *Opt. Express* **2015**, *23*, 32504.
[127] M. A. Meitl, E. Radauscher, R. Rotzoll, B. Raymond, S. Bonafede, D. Gomez, T. Moore, C. Prevatte, A. Fecioru, A. J. Trindade, C. A. Bower, *SID Symp. Dig. Tech. Pap.* **2017**, *48*, 257.
[128] K.-J. Chen, H. Chen, K.-A. Tsai, C. Lin, H.-H. Tsai, S.-H. Chien, B.-S. Cheng, Y.-J. Hsu, M.-H. Shih, C.-H. Tsai, H.-H. Shih, H.-C. Kuo, *Adv. Funct. Mater.* **2012**, *22*, 5138.
[129] H. E. Lee, D. Lee, T.-I. Lee, J. H. Shin, G.-M. Choi, C. Kim, S. H. Lee, J. H. Lee, Y. H. Kim, S.-M. Kang, S. H. Park, I.-S. Kang, T.-S. Kim, B.-S. Bae, K. J. Lee, *Nano Energy* **2019**, *55*, 454.
[130] K. Y. Kwon, H. Lee, M. Ghovanloo, A. Weber, W. Li, *2014 IEEE 27th Int. Conf. on Micro Electro Mechanical Systems (MEMS)* **2014**, 813.
[131] S. Il Park, D. S. Brenner, G. Shin, C. D. Morgan, B. A. Copits, H. U. Chung, M. Y. Pullen, K. N. Noh, S. Davidson, S. J. Oh, J. Yoon, K.-I. Jang, V. K. Samineni, M. Norman, J. G. Grajales-Reyes, S. K. Vogt, S. S. Sundaram, K. M. Wilson, J. S. Ha, R. Xu, T. Pan, T. Kim, Y. Huang, M. C. Montana, J. P. Golden, M. R. Bruchas, R. W. Gereau, J. A. Rogers, *Nat. Biotechnol.* **2015**, *33*, 1280.
[132] S. Y. Lee, K.-I. Park, C. Huh, M. Koo, H. G. Yoo, S. Kim, C. S. Ah, G. Y. Sung, K. J. Lee, *Nano Energy* **2012**, *1*, 145.
[133] J.-W. Jeong, J. G. McCall, G. Shin, Y. Zhang, R. Al-Hasani, M. Kim, S. Li, J. Y. Sim, K.-I. Jang, Y. Shi, D. Y. Hong, Y. Liu, G. P. Schmitz, L. Xia, Z. He, P. Gamble, W. Z. Ray, Y. Huang, M. R. Bruchas, J. A. Rogers, *Cell* **2015**, *162*, 662.
[134] A. H. Park, S. H. Lee, C. Lee, J. Kim, H. E. Lee, S. B. Paik, K. J. Lee, D. Kim, *ACS Nano* **2016**, *10*, 2791.
[135] M. Koo, S. Y. Park, K. J. Lee, *Nanobiosensors Dis. Diagn.* **2012**, *1*, 5.
[136] Y. C. Yang, J.-K. Sheu, M.-L. Lee, C. H. Yen, W.-C. Lai, S. J. Hon, T. K. Ko, *Opt. Express* **2012**, *20*, A1019.
[137] J. H. Park, H. E. Lee, C. K. Jeong, D. H. Kim, S. K. Hong, K.-I. Park, K. J. Lee, *Nano Energy* **2019**, *56*, 531.
[138] D. H. Kim, H. E. Lee, B. K. You, S. B. Cho, R. Mishra, I.-S. Kang, K. J. Lee, *Adv. Funct. Mater.* **2018**, *29*, 1806338.